A new class of exponential integrators for SDEs with multiplicative noise

Citation for published version:
Erdogan, U & Lord, GJ 2019, 'A new class of exponential integrators for SDEs with multiplicative noise', *IMA Journal of Numerical Analysis*, vol. 39, no. 2, pp. 820-846. https://doi.org/10.1093/imanum/dry008

Digital Object Identifier (DOI):
10.1093/imanum/dry008

Link:
Link to publication record in Heriot-Watt Research Portal

Document Version:
Peer reviewed version

Published In:
IMA Journal of Numerical Analysis

IMA Journal of Numerical Analysis (2018) Page 1 of 25
doi:10.1093/imanum/drn000

A new class of exponential integrators for SDEs with multiplicative noise

UTKU ERDOĞAN†
Uşak, Turkey.
AND
AND GABRIEL J. LORD‡
Department of Mathematics and Maxwell Institute for Mathematical Sciences,
Heriot Watt University,
EH14 4AS Edinburgh, U.K.

[Received on 16 January 2018]

In this paper, we present new types of exponential integrators for Stochastic Differential Equations (SDEs) that take advantage of the exact solution of (generalised) geometric Brownian motion. We examine both Euler and Milstein versions of the scheme and prove strong convergence, taking care to deal with the dependence on the noise in the solution operator. For the special case of linear noise we obtain an improved rate of convergence for the Euler version over standard integration methods. We investigate the efficiency of the methods compared with other exponential integrators for low dimensional SDEs and high dimensional SDEs arising from the discretisation of SPDEs. We show that, by introducing a suitable homotopy parameter, these schemes are competitive not only when the noise is linear but also in the presence of nonlinear noise terms. Although our new schemes are derived and analysed under zero commutator conditions (1.2), our numerical investigations illustrate that the resulting methods rival traditional methods even when this does not hold.

Keywords: SDEs, Exponential Integrator, Euler Maruyama, Exponential Milstein, Homotopy, Geometric Brownian Motion

1. Introduction

We develop new exponential integrators for the numerical approximation of stochastic differential equations (SDEs) of the following form

$$d\mathbf{u} = (A\mathbf{u} + \mathbf{F}(\mathbf{u}))\,dt + \sum_{i=1}^{m} (B_i\mathbf{u} + \mathbf{g}_i(\mathbf{u}))\,dW_i(t), \qquad \mathbf{u}(0) = \mathbf{u}_0 \in \mathbb{R}^d, \qquad m,d \in \mathbb{N} \tag{1.1}$$

where $W_i(t)$ are iid Brownian motions, $\mathbf{F}, \mathbf{g}_i : \mathbb{R}^d \to \mathbb{R}^d$, and the matrices $A, B_i \in \mathbb{R}^{dxd}$, satisfy the following zero commutator conditions

$$[A, B_i] = 0, \quad [B_j, B_i] = 0, \qquad \text{for} \quad i, j = 1 \ldots m. \tag{1.2}$$

There are many SDE systems that can be written in this form, for example two well known SDE systems are the FitzHugh-Nagumo equation with multiplicative noise Hasegawa (2008) and the Lotka–Volterra

†Email: utkuerdog@gmail.com
‡Email: g.j.lord@hw.ac.uk

system Li *et al.* (2009). In practice, this form of SDEs is also encountered after space discretisation of stochastic partial differential equations (SPDEs) with diagonal noise (see Section 4.2). We derive our schemes and prove convergence under the condition (1.2). On the other hand, we see below that our schemes remain consistent and are efficient even for non commutative matrices (see Section 4.3 and Section 4.4). In the deterministic setting, exponential integrators have proved to be very efficient for the numerical solution of stiff (partial) differential equations when compared to implicit solvers see, for example, the review in Hochbruck & Ostermann (2010). The derivation and usage of exponential integrators in the stochastic setting is still an active research area. Local linearisation methods were first proposed by Jimenez *et al.* (1999); Biscay *et al.* (1996) for SDEs with both additive and multiplicative noise. These methods continue to receive attention, for example Mora (2005); Jimenez & Carbonell (2015) examine weak approximation and Carbonell & Jimenez (2008) considers more general noise terms. Recently Komori & Burrage (2014) examined mean square stability of exponential integrators for semi-linear stiff SDEs. The method is the same basic one as developed for the space discretisations of SPDEs. For SPDEs with additive noise, Lord & Rougemont (2004) introduced an exponential scheme for stochastic PDEs that was later improved upon in Jentzen & Kloeden (2009); Kloeden *et al.* (2011). Jentzen and co-workers (see, e.g. Jentzen & Kloeden (2009); Jentzen (2009, 2010) and references there in) have further extended these results to include more general nonlinearities. There has been less work on exponential integrators with multiplicative noise. Strong convergence of stochastic exponential integrators for SDEs arising from the space discretisation of SPDEs by a finite element method is considered in Lord & Tambue (2012). More recently, a higher order exponential integrator of Milstein type was introduced by Jentzen & Röckner (2015).

All the above exponential integrators for SDEs (e.g. arising from the discretisation of the SPDEs) are based on the semi group operator $\mathbf{S}_{t,t_0} = \exp((t-t_0)A)$ obtained from the following linear equation

$$d\mathbf{S}_{t,t_0} = A\mathbf{S}_{t,t_0}dt, \qquad \mathbf{S}_{t_0,t_0} = I_d$$

where I_d is the unit matrix in $\mathbb{R}^{d\times d}$. For comparison, consider the following two standard exponential integrators for (1.1) with multiplicative noise: *SETD0*

$$\mathbf{u}_{n+1} = e^{\Delta tA}\left(\mathbf{u}_n + \mathbf{F}(\mathbf{u}_n)\Delta t + \sum_{i=1}^{m}\left(B_i\mathbf{u}_n + \mathbf{g}_i(\mathbf{u}_n)\right)\Delta W_{i,n}\right) \tag{1.3}$$

and *SETD1*

$$\mathbf{u}_{n+1} = e^{\Delta tA}\left(\mathbf{u}_n + \sum_{i=1}^{m}\left(B_i\mathbf{u}_n + \mathbf{g}_i(\mathbf{u}_n)\right)\Delta W_{i,n}\right) + \varphi(\Delta tA)\mathbf{F}(\mathbf{u}_n)\Delta t, \tag{1.4}$$

where

$$\varphi(A) = A^{-1}\left(\exp(A) - I_d\right), \qquad \Delta t = t_{n+1} - t_n, \qquad \text{and} \qquad \Delta W_{i,n} = W_i(t_{n+1}) - W_i(t_n).$$

These methods are essentially exact for a linear system of ODEs. We extend this approach to take advantage of the known solution of geometric Brownian motion in the numerical approximation. To do this, we consider the linear homogeneous matrix differential equation

$$d\Phi_{t,t_0} = A\Phi_{t,t_0}dt + \sum_{i=1}^{m} B_i\Phi_{t,t_0}dW_i(t), \qquad \Phi_{t_0,t_0} = I_d \tag{1.5}$$

and construct new schemes that are exact for a class of linear multiplicative SDEs of this form.

In the next section we derive our new exponential integrators for multiplicative noise and introduce the homotopy scheme. The main results of strong convergence analysis for the Euler and Milstein versions of the scheme are stated in Section 3 and for linear noise we obtain a strong rate of $\mathscr{O}(\Delta t)$ convergence for our Euler type scheme, improving over standard methods in this case. In addition we comment on mean-square stability in this section. Numerical examples are presented to examine the efficiency of the proposed schemes. We consider an SDE and a discretised SPDE where the commutator conditions (1.2) hold before looking at SDEs and a discretised SPDE where they do not. We see that in all the cases examined that the new schemes are competitive. Section 5 contains the proofs of strong convergence of $\mathscr{O}(\Delta t^{1/2})$ for the Euler version and $\mathscr{O}(\Delta t)$ for the Milstein version of our methods and finally we conclude.

2. Derivation of the methods

Throughout we assume that $T \in (0,\infty)$ is a fixed real number and we have a partition of the time interval $[0,T]$, $0 = t_0 < t_1 < t_2 < \ldots < t_N = T$ with constant step size $\Delta t = t_{j+1} - t_j$. Let $(\Omega, \mathscr{F}, \mathbb{P})$ be a probability space with filtration $(\mathscr{F}_t)_{t\in[0,T]}$. Then under suitable assumptions on $\mathbf{F}$ and $\mathbf{g}_i$ it is well known that there exists an $\mathscr{F}_{t^-}$ adapted stochastic process $u : [0,T] \times \Omega \to \mathbb{R}^d$ satisfying (1.1), Mao (1997); Øksendal (2003); Lord *et al.* (2014). The linear homogeneous matrix differential equation (1.5) has the exact solution

$$\Phi_{t,t_0} = \exp\left((A - \frac{1}{2}\sum_{i=1}^{m} B_i^2)(t-t_0) + \sum_{i=1}^{m} B_i (W_i(t) - W_i(t_0)) \right).$$

Let $\mathbf{u}(t)$ be the solution of (1.1) and take $t = t_{n+1}$, $t_0 = t_n$. Then, applying the Ito formula to $\mathbf{Y}(t) = \Phi_{t,t_0}^{-1}\mathbf{u}$, we obtain

$$\mathbf{u}(t_{n+1}) = \Phi_{t_{n+1},t_n}\left(\mathbf{u}(t_n) + \int_{t_n}^{t_{n+1}} \Phi_{s,t_n}^{-1}\tilde{f}(\mathbf{u}(s))\,ds \;+ \sum_{i=1}^{m}\int_{t_n}^{t_{n+1}} \Phi_{s,t_n}^{-1}\mathbf{g}_i(\mathbf{u}(s))dW_i(s)\right) \tag{2.1}$$

where

$$\tilde{\mathbf{f}}(.) = \mathbf{F}(.) - \sum_{i=1}^{m} B_i \mathbf{g}_i(.). \tag{2.2}$$

Different treatment of the integrals in (2.1) leads to different numerical schemes. We examine Euler and Milstein type methods here, although clearly higher order methods, such as Wagner-Platen type schemes (see for example Becker *et al.* (2016)) could be developed. Derivation of the methods below use the commutativity of the matrices in (1.2). This condition does not hold in general. However, it is straightforward to show by an Ito-Taylor expansion consistency of the methods for the non-commutative case. Numerically we observe that the accompanying error is small (see Section 4.3 and Section 4.4). First we derive Euler type Exponential Integrators and then in Section 2.2 turn to Milstein versions.

2.1 *Euler type Exponential Integrators*

We take the following approximation for the stochastic integral in (2.1)

$$\Phi_{t_{n+1},t_n}\int_{t_n}^{t_{n+1}} \Phi_{s,t_n}^{-1}\mathbf{g}_i(\mathbf{u}(s))dW_i(s) \approx \Phi_{t_{n+1},t_n}\mathbf{g}_i(\mathbf{u}(t_n))\Delta W_{i,n} \tag{2.3}$$

where $\Delta W_{i,n} = W_i(t_{n+1}) - W_i(t_n)$ and we derive Euler type Exponential Integrators below. For the deterministic integral in (2.1) we examine three cases.

1. Taking $\Phi_{t_{n+1},t_n} \int_{t_n}^{t_{n+1}} \Phi_{s,t_n}^{-1} \tilde{\mathbf{f}}(\mathbf{u}(s))ds \approx \Phi_{t_{n+1},t_n} \tilde{\mathbf{f}}(\mathbf{u}(t_n))\Delta t$, we obtain our first method *EI0*
$$\mathbf{u}_{n+1} = \Phi_{t_{n+1},t_n} \left(\mathbf{u}_n + \tilde{\mathbf{f}}(\mathbf{u}_n)\Delta t + \sum_{i=1}^{m} \mathbf{g}_i(\mathbf{u}_n)\Delta W_{i,n} \right).$$

2. If we take $\Phi_{t_{n+1},s} \int_{t_n}^{t_{n+1}} \Phi_{s,t_n}^{-1} \tilde{\mathbf{f}}(\mathbf{u}(s))ds \approx \mathbf{Z}_{t_{n+1},t_n} \varphi(\Delta t A) \tilde{\mathbf{f}}(\mathbf{u}(t_n))\Delta t$ where
$$\mathbf{Z}_{t,s} = \exp\left(-\frac{1}{2}\sum_{i=1}^{m} B_i^2 (t-s) + \sum_{i=1}^{m} B_i (W_i(t) - W_i(s)) \right)$$
then we obtain our second method *EI1*
$$\mathbf{u}_{n+1} = \Phi_{t_{n+1},t_n} \left(\mathbf{u}_n + \sum_{i=1}^{m} \mathbf{g}_i(\mathbf{u}_n)\Delta W_{i,n} \right) + \mathbf{Z}_{t_{n+1},t_n} \varphi(\Delta t A) \tilde{\mathbf{f}}(\mathbf{u}_n)\Delta t.$$

3. Finally with $\Phi_{t_{n+1},t_k} \int_{t_n}^{t_{n+1}} \Phi_{s,t_n}^{-1} \tilde{\mathbf{f}}(\mathbf{u}(s))ds \approx \varphi(\Delta t A) \tilde{\mathbf{f}}(\mathbf{u}(t_n))\Delta t$ we get the method *EI2*
$$\mathbf{u}_{n+1} = \Phi_{t_{n+1},t_n} \left(\mathbf{u}_n + \sum_{i=1}^{m} \mathbf{g}_i(\mathbf{u}_n)\Delta W_{i,n} \right) + \varphi(\Delta t A) \tilde{\mathbf{f}}(\mathbf{u}_n)\Delta t.$$

We focus on *EI0*, however we compare the accuracy and efficiency of these approximations in Section 4. For general noise the schemes *EI0*, *EI1*, *EI2* all have the same strong rate of convergence as *SETD0* in (1.3) and *SETD1* (1.4) which is $\mathscr{O}(\Delta t^{1/2})$. However, we expect an improvement in the error when the terms in B_i dominate $\mathbf{g}_i$ in the noise. In the special case where $\mathbf{g}_i \equiv 0$ we prove, and show numerically, an improvement in the strong rate of convergence to $\mathscr{O}(\Delta t)$.

It should be noted that all the proposed new type integrators reduce to the usual exponential integrators *SETD0* and *SETD1* when $B_i = 0$, $i = 1 \dots m$. Indeed, it is observed in numerical simulations that *SETD* schemes may perform better than the new *EI* schemes when the B_i are small compared to $\mathbf{g}_i$. On the other hand the *EI* schemes outperform *SETD* schemes when B_i are dominant. We can capture the good properties of both methods by introducing a homotopy parameter $p \in [0,1]$. Let us rewrite (1.1) as
$$d\mathbf{u} = (A\mathbf{u} + \mathbf{F}(\mathbf{u}))\,dt + \sum_{i=1}^{m} (pB_i\mathbf{u} + [\mathbf{g}_i(\mathbf{u}) + (1-p)B_i\mathbf{u}])\,dW_i(t). \tag{2.4}$$
For example, applying *EI0* for this equation, one obtains *HomEI0*
$$\mathbf{u}_{n+1} = \Phi^p_{t_{n+1},t_n} \left(\mathbf{u}_n + \tilde{\mathbf{f}}^p(\mathbf{u}_n)\Delta t + \sum_{i=1}^{m} \mathbf{g}_i^p(\mathbf{u}_n)\Delta W_{i,n} \right) \tag{2.5}$$
where
$$\Phi^p_{t_{n+1},t_n} = \exp\left((A - \frac{1}{2}\sum_{i=1}^{m} p^2 B_i^2)\Delta t + \sum_{i=1}^{m} pB_i \Delta W_i, n \right), \tag{2.6}$$
$$\mathbf{g}_i^p(\mathbf{u}) = \mathbf{g}_i(\mathbf{u}) + (1-p)B_i\mathbf{u}, \quad \text{and} \quad \tilde{\mathbf{f}}^p(\mathbf{u}) = \mathbf{F}(\mathbf{u}) - \sum_{i=1}^{m} pB_i\mathbf{g}_i^p(\mathbf{u}). \tag{2.7}$$

It is clear that $p=0$ and $p=1$ give *SETD0* and *EI0* respectively. In Section 4 we suggest a fixed formula for p based on the weighting of B_i to $\mathbf{g}_i$ (see (4.2)). However, further consideration could be given to an optimal choice of either a fixed p or of a p assigned during the computation by considering weights of the terms in the diffusion coefficient, so that $p(u,B_i,g_i)$. We note that unlike Milstein methods, *HomEI0* and the other *EI* methods have the advantage that they do not require the derivative of the diffusion term.

2.2 *Milstein type Exponential Integrators*

An alternative treatment of (2.1) is to use the Ito-Taylor expansion of the diffusion term

$$\Phi_{s,t_n}^{-1}\mathbf{g}_i(\mathbf{u}(s)) = \mathbf{g}_i(\mathbf{u}(t_n)) + \sum_{l=1}^{m}\int_{t_n}^{s}\Phi_{r,t_n}^{-1}\mathbf{H}_{i,l}(\mathbf{u}(r))dW_l(r) + \int_{t_n}^{s}\Phi_{r,t_n}^{-1}\mathbf{Q}_i(\mathbf{u}(r))dr \tag{2.8}$$

where

$$\mathbf{H}_{i,l}(\mathbf{u}(.)) = D\mathbf{g}_i(\mathbf{u}(.))(B_l\mathbf{u}(.) + \mathbf{g}_l(\mathbf{u}(.))) - B_l\mathbf{g}_i(\mathbf{u}(.)) \tag{2.9}$$

and $\mathbf{Q}_i(.)$ is the vector function in terms of $A, \mathbf{F}, D\mathbf{g}_i, D^2\mathbf{g}_i$, B_l for $i,l = 1,...,m$ (which, for ease of presentation, we do not detail here).

Freezing the integrand of stochastic integral at $r = t_n$ and dropping the deterministic integral

$$\Phi_{s,t_n}^{-1}\mathbf{g}_i(\mathbf{u}(s)) = \mathbf{g}_i(\mathbf{u}(t_n)) + \sum_{l=1}^{m}\int_{t_n}^{s}\mathbf{H}_{i,l}(\mathbf{u}(t_n))dW_l(r) + h.o.t \tag{2.10}$$

then dropping the higher order terms, we obtain the Milstein scheme *MI0*

$$\mathbf{u}_{n+1} = \Phi_{t_{n+1},t_n}\left(\mathbf{u}_n + \tilde{\mathbf{f}}(\mathbf{u}_n)\Delta t + \sum_{i=1}^{m}\mathbf{g}_i(\mathbf{u}_n)\Delta W_{i,n} + \sum_{i=1}^{m}\sum_{l=1}^{m}\mathbf{H}_{i,l}(\mathbf{u}_n)\int_{t_n}^{t_{n+1}}\int_{t_n}^{s}dW_l(r)dW_i(s)\right) \tag{2.11}$$

where $\tilde{\mathbf{f}}$ is defined as in (2.2). We also introduce a Milstein homotopy type scheme *HomMI0* by applying *MI0* to (2.4).

3. Strong convergence and mean-square stability

We state in this section the strong convergence result for both *EI0* and *MI0*. Proofs are given in Section 5 and we note that the proofs for the other schemes, including those such as (2.5), are similar. For these proofs we assume a global Lipschitz condition on the drift and diffusion although tamed versions of the methods for more general drift and diffusions can be derived. We let $\|\cdot\|_2$ denote the standard Euclidean norm for both vectors and matrices and $\|\cdot\|^2_{L^2(\Omega,\mathbb{R}^d)} = \mathbb{E}\left[\|\cdot\|_2^2\right]$.

Assumption 1 There exists a constant $L > 0$ such that the linear growth condition holds: for $\mathbf{u} \in \mathbb{R}^d$ and $i = 1,\ldots,m$

$$\|\mathbf{F}(\mathbf{u})\|_2^2 \leqslant L(1+\|\mathbf{u}\|_2^2), \qquad \|\mathbf{g}_i(\mathbf{u})\|_2^2 \leqslant L(1+\|\mathbf{u}\|_2^2),$$

and the global Lipschitz condition holds: for $\mathbf{u},\mathbf{v} \in \mathbb{R}^d$, $i = 1,\ldots,m$

$$\|\mathbf{F}(\mathbf{u}) - \mathbf{F}(\mathbf{v})\|_2 \leqslant L\|\mathbf{u}-\mathbf{v}\|_2, \qquad \|\mathbf{g}_i(\mathbf{u}) - \mathbf{g}_i(\mathbf{v})\|_2 \leqslant L\|\mathbf{u}-\mathbf{v}\|_2.$$

First we state the strong convergence result for the Euler type scheme *EI0*.

THEOREM 3.1 Let Assumptions 1 hold and let $\mathbf{u}_n$ be the approximation to the solution of (1.1) using *EI0*. Then, for $T > 0$, there exists $K > 0$ independent of Δt such that

$$\sup_{0 \leqslant t_n \leqslant T} \|\mathbf{u}(t_n) - \mathbf{u}_n\|_{L^2(\Omega,\mathbb{R}^d)} \leqslant K\Delta t^{1/2}. \tag{3.1}$$

For the Milstein scheme *MI0*, we impose the following two extra assumptions.

Assumption 2 The functions $F, \mathbf{g}_i : \mathbb{R}^d \to \mathbb{R}^d$ are twice continuously differentiable.

Assumption 3 For the same constant L as in Assumption 1 for $\mathbf{u}, \mathbf{v} \in \mathbb{R}^d$, $i, l = 1, \ldots, m$

$$\|D\mathbf{g}_i(\mathbf{u})\mathbf{g}_l(\mathbf{u}) - D\mathbf{g}_i(\mathbf{v})\mathbf{g}_l(\mathbf{v})\|_2 \leqslant L\|\mathbf{u} - \mathbf{v}\|_2$$

and

$$\|D\mathbf{g}_i(\mathbf{u})B_l\mathbf{u} - D\mathbf{g}_i(\mathbf{v})B_l\mathbf{v}\|_2 \leqslant L\|\mathbf{u} - \mathbf{v}\|_2\,.$$

THEOREM 3.2 Let Assumptions 1, 2 and 3 hold and let $\mathbf{u}_n$ be the approximation to the solution of (1.1) using *MI0*. Then, for $T > 0$, there exists $K > 0$ independent of Δt such that

$$\sup_{0 \leqslant t_n \leqslant T} \|\mathbf{u}(t_n) - \mathbf{u}_n\|_{L^2(\Omega,\mathbb{R}^d)} \leqslant K\Delta t. \tag{3.2}$$

Note that from the definition of $\tilde{\mathbf{f}}$ in (2.2) and $\mathbf{H}_{i,l}$ in (2.9), these functions also satisfy global Lipschitz and/or continuously differentiability conditions when the corresponding assumptions on $\mathbf{F}$, $\mathbf{g}_i$ and $D\mathbf{g}_i$ hold. We give the proofs of Theorem 3.1 and Theorem 3.2 in Section 5.

Now consider the special case when $\mathbf{g}_i \equiv 0$ in (1.1). Namely, we have the SDE

$$d\mathbf{u} = (A\mathbf{u} + \mathbf{F}(\mathbf{u}))\,dt + \sum_{i=1}^{m} B_i\mathbf{u}dW_i(t), \qquad \mathbf{u}(0) = \mathbf{u}_0 \in \mathbb{R}^d, \tag{3.3}$$

for which both the numerical schemes *EI0* and *MI0* reduce to

$$\mathbf{u}_n = \Phi_{t_{n+1},t_n}(\mathbf{u}_n + \mathbf{F}(\mathbf{u}_n)\Delta t)\,. \tag{3.4}$$

Remark that we can consider (3.4) as a Lie-Trotter splitting of (3.3). It is straightforward to conclude the following improvement in the convergence rate for *EI0*.

COROLLARY 3.1 Suppose that Assumption 1 holds and $\mathbf{F}$ is continuously differentiable. Let $\mathbf{u}_n$ denote the approximation to the solution of (3.3) by (3.4). Then for $T > 0$, there exists $K > 0$ independent of Δt such that

$$\sup_{0 \leqslant t_n \leqslant T} \|\mathbf{u}(t_n) - \mathbf{u}_n\|_{L^2(\Omega,\mathbb{R}^d)} \leqslant K\Delta t. \tag{3.5}$$

This is a simple consequence of solving the linear SDE exactly, see Section 5.

3.1 *Mean-Square stability of HomEI0*

The standard one dimensional SDE used to examine mean square stability is given by

$$du = \lambda u dt + \mu u dW, \qquad u(0) = u_0 \in \mathbb{R} \tag{3.6}$$

where λ and μ are allowed to be complex, see for example (Saito & Mitsui, 1996; Komori & Burrage, 2014; Buckwar & Kelly, 2010). Assuming $u_0 \neq 0$, then the exact solution $u(t)$ of (3.6) satisfies

$$\lim_{t\to\infty} \mathbb{E}|u(t)|^2 = 0 \quad \text{if and only if} \quad \mathscr{R}\{\lambda\} + \frac{1}{2}|\mu|^2 < 0.$$

The proposed method *EI0* exactly solves (3.6) and its stability region is given by

$$\hat{R}_{EI0} = \left\{ (z_1, z_2) \quad | \quad z_1 + \frac{1}{2} z_2 < 0 \right\}$$

where $z_1 = \mathscr{R}(\lambda)\Delta t$ and $z_2 = |\mu|^2 \Delta t$. To determine the stability region of $HomEI0$ method, we apply *EI0* to the test equation (3.6) in the following form

$$du = \lambda u dt + (p\mu u + (1-p)\mu u)\, dW, \qquad u(0) = u_0.$$

We obtain the stability region

$$\hat{R}_{HomEI0} = \left\{ (z_1, z_2) \quad | \quad e^{2z_1 + p^2 z_2} \left(1 + z_2(1-p^2) + z_2^2 p^2 (p-1)^2\right) < 1 \right\}$$

where the cases $p = 0$ and $p = 1$ correspond to *SETD0* and *EI0* respectively. Therefore, the stability region of *HomEI0* shrinks continuously as p changes from 0 to 1 and $\hat{R}_{EI0} \subset \hat{R}_{HomEI0} \subset \hat{R}_{SETD0}$. This is illustrated in Figure 3.1.

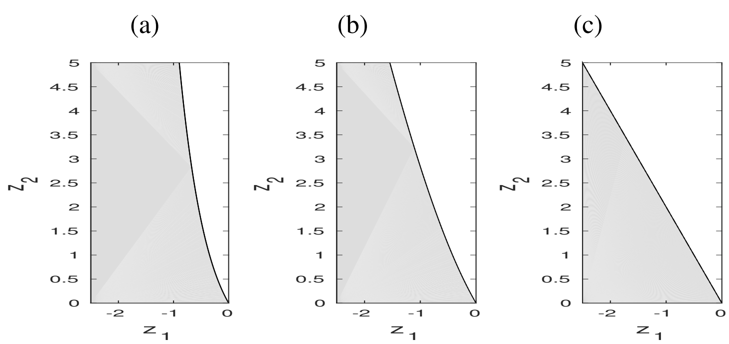

FIG. 1. Mean-square stability regions for *HomEI0* with (a) $p = 0$ (*SETD0*), (b) $p = 1/2$ and (c) $p = 1$ (*EI0*).

4. Numerical examples

In this section we perform some numerical experiments to illustrate and confirm the orders of the proposed methods. For comparison *SETD0*, *SETD1*, Exponential Milstein *ExpMIL* Jentzen & Röckner (2015), the classical Milstein Kloeden & Platen (2011) are used as well as the semi-implicit Euler–Maruyama scheme (EM). We consider SDEs of the form of (1.1) and in particular we introduce two parameters α and β so that we have

$$d\mathbf{u} = (A\mathbf{u} + \mathbf{F}(\mathbf{u}))\, dt + \sum_{i=1}^{m} (\beta B_i \mathbf{u} + \alpha \mathbf{g}_i(\mathbf{u}))\, dW_i(t), \qquad \mathbf{u}(0) = \mathbf{u}_0 \in \mathbb{R}^d \qquad m, d \in \mathbb{N}. \tag{4.1}$$

When $\alpha \ll \beta$ the linear terms B_i dominate, whereas if $\alpha \gg \beta$, the nonlinearity $\mathbf{g}_i$ dominates. By examining different α and β we can see the effect of the strength of the nonlinearity.

For *HomEI0* and *HomMI0* we define the homotopy parameter by

$$p = \frac{|\beta|}{|\alpha| + |\beta|}. \tag{4.2}$$

Where we do not have an exact solution below we compute a reference solution using the exponential Milstein method with a small step size Δt_{ref} and examine a Monte Carlo estimate of $\|\mathbf{u}(t_n) - \mathbf{u}_n\|_{L^2(\Omega,\mathbb{R}^d)}$, the root mean square error (RMSE), with M realisations. In Section 4.1 and Section 4.2 the commutativity conditions (1.2) hold unlike our examples in Section 4.3 and Section 4.4.

4.1 *The Ginzburg-Landau equation*

Consider the one dimensional equation

$$du(t) = \left(-u + \frac{\sigma}{2}u - u^3\right)dt + \sqrt{\sigma}u dW(t), \qquad u(0) = u_0 \tag{4.3}$$

that has exact solution Kloeden & Platen (2011)

$$u(t) = \frac{u_0 e^{-t+\sqrt{\sigma}W(t)}}{\sqrt{1 + 2u_0^2 \int_0^t e^{-2s+2\sqrt{\sigma}W(s)}ds}}. \tag{4.4}$$

It should be noted that the drift term satisfies only a one sided global Lipschitz condition and our proposed schemes can be tamed to guarantee strong convergence as in Hutzenthaler & Jentzen (2015). Nevertheless, simulations reveal the performance of the new schemes *EI0*, *EI1* and *EI2* and act as a benchmark for *SETD1* (see also Jentzen & Röckner (2015)). Note that (4.3) is linear in the diffusion and hence Corollary 3.1 holds and we expect first order convergence and *MI0* and *HomMI0* both reduce to *EI0* and *HomEI0*. This is observed numerically in Figure 2 (a) where we see first order convergence of the methods *EI0*, *EI1* and *EI2*. In Figure 2 (b) we compare the efficiency of the schemes and observe that *EI0* is the most efficient. From now on we no longer consider *EI1* or *EI2*.

4.2 *A spectral Galerkin discretisation of an SPDE*

We examine the strong convergence of the schemes *EI0*, *HomEI0* applied to SDEs arising from the spectral Galerkin discretisation in space of an SPDE. Consider the stochastic reaction-diffusion equation

$$du = \left[\varepsilon \frac{\partial^2 u}{\partial x^2} + 1 - u\right]dt + \left[\beta u + \alpha \frac{1-u}{1+u^2}\right]dW(t), \qquad u(x,0) = u_0(x) = \sin(\pi x), \tag{4.5}$$

with $x \in [0,1]$ subject to zero Dirichlet boundary conditions. We take $W(t)$ to be a Q–Wiener process and let Q have orthonormal eigenfunctions $g_j(x) = \sqrt{2}sin(j\pi x)$ and eigenvalues $\nu_j = \frac{1}{j^2}$, $j \in \mathbb{N}$, so that

$$W(t) = \sum_{j\in\mathbb{N}} \frac{1}{j} g_j \beta_j(t),$$

where $\beta_j(t)$ are iid Brownian motions. Applying the spectral Galerkin method as described for example in Jentzen & Röckner (2015) to discretise in space, we implement *EI0* in Algorithm 1. In the notation

(a) (b)

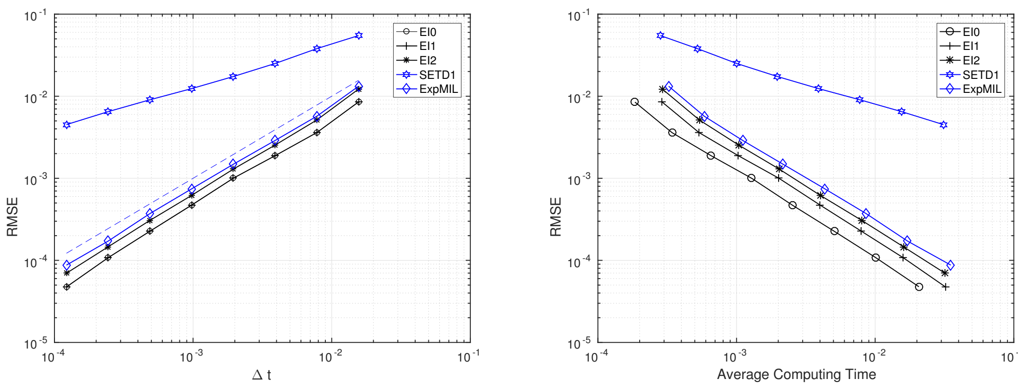

FIG. 2. Stochastic Ginzburg-Landau Equation (4.3) with $\sigma = 2$, $T = 1$, $M = 1000$ samples (a) root mean square error against Δt. Also plotted is a reference line with slope 1. (b) root mean square error against cputime. Of the new schemes *EI0* is the most efficient. We observe the improved convergence rate of Corollary 3.1 in these new schemes over that for *SETD1*.

of (1.1) for the SDEs after spatial discretisation the commutator conditions (1.2) hold. We note that Jentzen and Röckner derived the special case of *EI0* for $\alpha = 0$ in Jentzen & Röckner (2015) as a splitting procedure. However, they employed SETD schemes without computing exponentials of diffusion coefficients for non zero α values. In Figure 3 we show convergence (a) and efficiency (b) of the method *EI0* compared to EM and *SETD0* with $\beta = 1$ and $\alpha = 0$. By our choice of p in (4.2) with $\alpha = 0$ the scheme *HomEI0* reduces to *EI0*. In Figure 4 we include nonlinearity and take $\alpha = 1$. The linear and non linear terms are equally weighted and we see that *HomEI0* is more efficient than the standard integrators.

(a) (b)

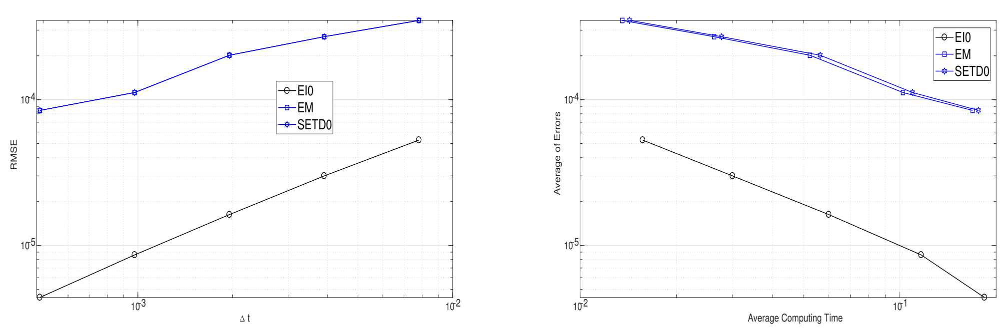

FIG. 3. Equation (4.5) with $\varepsilon = 0.01$, $T = 1$ and $M = 1000$ samples with $\beta = 1$, $\alpha = 0$, for which *HomEI0* and *EI0* are the same and the noise consists of a linear diagonal term. In (a) we show the root mean square error against Δt and in (b) root mean square error against cputime. We observe that *EI0* is the most efficient.

Algorithm 1 Script to solve (4.5) by using *EI0* combined with a spectral Galerkin method.

```
N=pow2(18);T=1.0;Dt=T/N; %number of steps,final time,step size
d=128;J=[1:d]'; %spatial discreitzation
A=-pi^2*J.^2/100; mu=J.^(-2); % linear operator and e.val for noise
y=sin(pi*J/(d+1)); Y=idst(y)/sqrt(2); % initial data
beta=1;alpha=0.1;    % problem parameters
b=@(x)  alpha*(1-x)./(1+x.^2); % set functions
f=@(x) 1-x;
g=zeros(d,1);
for j=1:d
 g=g+2*sin(j*J./(d+1)*pi).^2*mu(j);
end
for j=1:N  % loop over time steps
  y=dst(Y)*sqrt(2); % get discrete sine transform
  dW=dst(randn(d,1).*sqrt(Dt*mu*2)); % get increment for noise
  % update step
  y=exp(-beta^2/2*g*Dt+beta*dW).*( y+(f(y)-beta.*g.*b(y))*Dt+b(y).*dW);
  Y=exp(Dt*A).*idst(y)/sqrt(2);
end
```

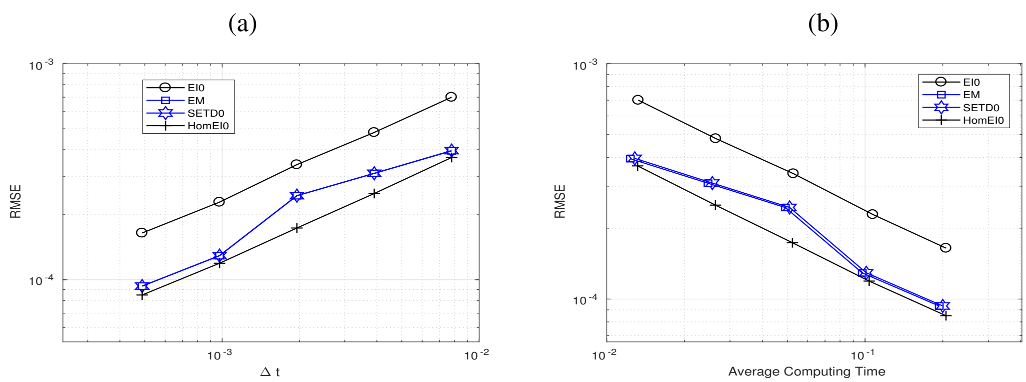

FIG. 4. Equation (4.5) with $\varepsilon = 0.01$, $T = 1$ and $M = 1000$ samples with $\beta = 1$, $\alpha = 1$. In (a) we show the root mean square error against Δt and in (b) the root mean square error against cputime. We see that *HomEI0* is the most efficient.

4.3 *Non-commutativity and nonlinear noise*

Consider the following SDE in $\mathbb{R}^4$, with initial data $\mathbf{u}(0) = (1,1,1,1)^T$

$$d\mathbf{u} = (rA\mathbf{u} + \mathbf{F}(\mathbf{u}))\,dt + G(\mathbf{u})d\mathbf{W}(t), \qquad F_j = \frac{u_j}{1+|u_j|}, \tag{4.6}$$

where r is a constant (we take $r=4$) and A arises from the standard finite difference approximation of the Laplacian

$$A=\begin{pmatrix}-2 & 1 & 0 & 0\\ 1 & -2 & 1 & 0\\ 0 & 1 & -2 & 1\\ 0 & 0 & 1 & -2\end{pmatrix}. \tag{4.7}$$

For a general matrix B we have $[A,B]\neq 0$ and the commutator conditions (1.2) will not hold below. However, it is straightforward to show by an Ito-Taylor expansion consistency of the methods and we show numerically below that the accompanying error is small.

Diagonal noise

First we look at diagonal noise and examine the effective of the noise being dominated by either linear or nonlinear terms. For the nonlinear part we let $g(u)=1/(1+u^2)$ and let $\mathbf{g}_i(\mathbf{u})$ have only one non-zero element $\alpha g(u_i)$ in the ith entry for $\alpha\in\mathbb{R}$. For the linear part we take $B_i=\beta diag(\mathbf{e}_i)$ where $\mathbf{e}_i$ is the ith unit vector of $\mathbb{R}^4$ and $\beta\in\mathbb{R}$ and as noted above $[A,B_i]\neq 0$. This gives $G(u)$ in (4.6) as

$$G(\mathbf{u})=\begin{pmatrix}\beta u_1+\alpha g(u_1) & 0 & 0 & \\ 0 & \beta u_2+\alpha g(u_2) & 0 & 0\\ 0 & 0 & \beta u_3+\alpha g(u_3) & 0\\ 0 & 0 & 0 & \beta u_4+\alpha g(u_4)\end{pmatrix}.$$

A script to implement *HomEI0* is presented in Algorithm 2. We show results for the both the Euler and Milstein type schemes for different α and β values with a reference step size $\Delta t_{\text{ref}}=2^{-20}$. First

Algorithm 2 Script to solve (4.6) with noise given by (4.3) using *HomEI0*

```
N=pow2(10);T=1.0;Dt=T/N;%number of steps,final time,step size
d=4;m=4; % dimension of problem and dimension of noise
r=4;beta=1;alpha=0.1; % parameters  of the problem
X=ones(d,1); %initial Condition
p=abs(beta)/(abs(beta)+abs(alpha));%set homotopy parameter
% Set Matrices
A=-r*sparse(toeplitz([2 -1 zeros(1, d-2)])); M1=expm(Dt*A);
% Set functions
f=@(u) u./(1+abs(u)); g=@(u) 1./(1+u.^2);
ftilde=@(u) f(u)-p*beta*(alpha*g(u)+(1-p)*beta*u);
Gtilde=@(u) alpha*g(u)+ (1-p)*beta*u;
for n=1:N   % loop over time steps
  dW = sqrt(Dt)*randn(m,1);  % get increment for noise
  M2 = exp(-Dt*0.5*p^2*beta^2+p*beta*dW);
  X=M1*M2.*(X+Dt*ftilde(X)+Gtilde(X).*dW);  % update step
end
```

consider the case where $\alpha=0.1$ and $\beta=1$ so that the linear term dominates. Figure 5 (a) illustrates orders and (b) the efficiency of the methods *EI0*, *SETD0*, *HomEI0*. In Figure 5 (a) we see convergence with the predicted rate and in Figure 5 (b) it is clear that *EI0* and *HomEI0* are more efficient than either *SETD0* or the semi-implicit Euler–Maruyama method (EM). Recall that if $\alpha=0$ then we obtain first order convergence for *EI0* and *HomEI0* which is not the case for *SETD0* or EM. Figure 6 (a) shows first order convergence for the Milstein schemes and from (b) we see that *HomMI0* and *MI0* are the most efficient. However, when $\beta = \alpha = 1$ (and we have equal weighting between the linear and nonlinear

(a) (b)

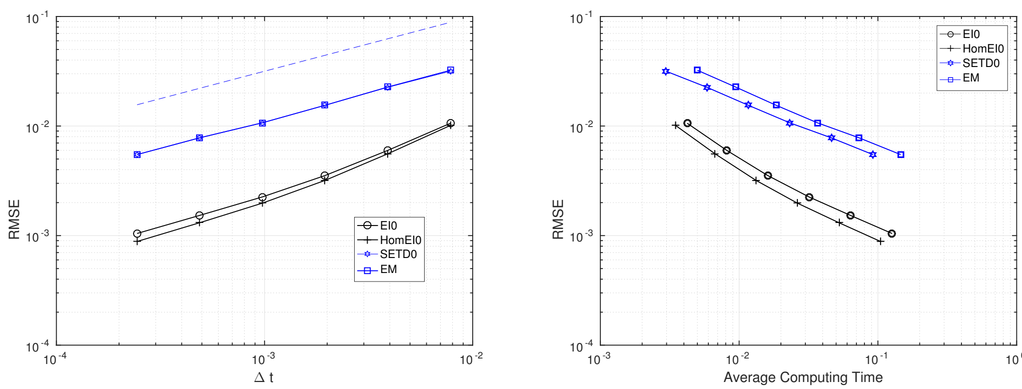

FIG. 5. Euler methods. Equation (4.6) $\beta = 1$, $\alpha = 0.1$, $r = 4$, $T = 1$ and $M = 1000$ samples (a) root mean square error against Δt. Also plotted is a reference line with slope 1/2. (b) root mean square error against cputime. Here the linear noise term dominates and we see *HomEI0* is the most efficient, followed by *EI0*. See Figure 6 for Milstein schemes.

term) we see in Figure 7 (a) the same rate of convergence but now *HomEI0* is more accurate than *EI0* and from Figure 7 (b) that *HomEI0* is still the most efficient, followed by *SETD0*. This illustrates the effectiveness of adding the homotopy parameter. For the Milstein schemes we see the predicted rate of convergence in Figure 8 (a) and in (b) that *HomEI0* and *MI0* are very marginally more efficient than either the classical Milstein or Exponential Milstein schemes.

In Figure 9 we have $\beta = 0.1$ and $\alpha = 1$ so that it is the nonlinearity that dominates. We now see that the errors from *HomEI0* are similar to those or the standard integrators *SETD0* and EM and that *SETD0* is now more efficient. We note, however, that *HomEI0* remains more efficient than EM. For the Milstein schemes we see the predicted rate of convergence in Figure 10 (a) and in (b) that *HomEI0* and *MI0* are more efficient than either the classical Milstein or Exponential Milstein schemes.

Non-diagonal noise

Now consider (4.6) with non-commutative noise by taking the following diffusion coefficient matrix

$$G(\mathbf{u}) = \begin{pmatrix} \beta u_1 & 0 & 0 & \\ 0 & \beta u_2 - \alpha u_1 & 0 & 0 \\ 0 & 0 & \beta u_3 - \alpha u_2 & 0 \\ 0 & 0 & 0 & \beta u_4 - \alpha u_3 \end{pmatrix} \tag{4.8}$$

In order to apply *EI* schemes, consider the splitting

$$G(\mathbf{u}) = \beta \begin{pmatrix} u_1 & 0 & 0 & 0 \\ 0 & u_2 & 0 & 0 \\ 0 & 0 & u_3 & 0 \\ 0 & 0 & 0 & u_4 \end{pmatrix} - \alpha \begin{pmatrix} 0 & 0 & 0 & 0 \\ 0 & u_1 & 0 & 0 \\ 0 & 0 & u_2 & 0 \\ 0 & 0 & 0 & u_3 \end{pmatrix} \tag{4.9}$$

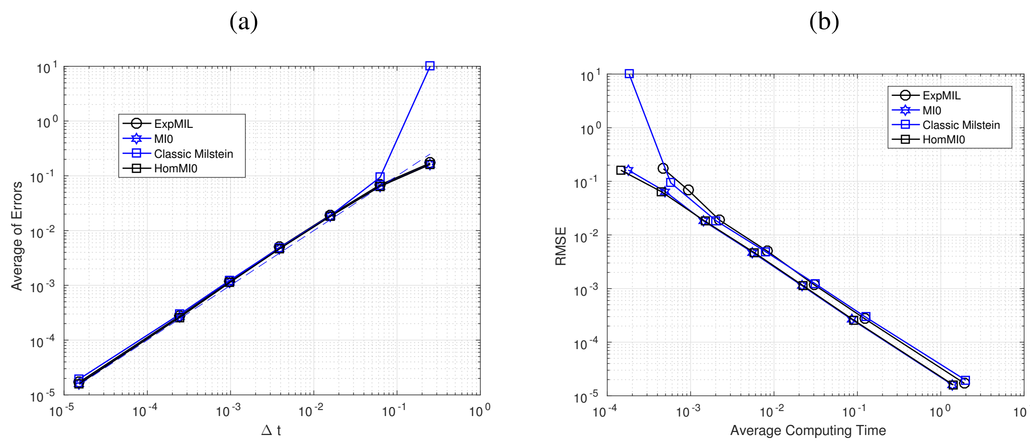

FIG. 6. Milstein methods. Equation (4.6) with $\beta = 1$, $\alpha = 0.1$, $r = 4$, $T = 1$ and $M = 100$ samples (a) root mean square error against Δt. Also plotted is a reference line with slope 1 (compare to Figure 5). In (b) root mean square error against cputime. Here the linear noise term dominates and we see *HomMI0* and *MI0* are the most efficient.

that gives the matrices $B_i = \beta diag(\mathbf{e}_i)$ and the vectors $\mathbf{g}_i(\mathbf{u})$ having only non zero element $-\alpha u_i$ in $(i-1)$ th entry. In this case Levy areas are now needed to apply the exponential Milstein scheme. We take a reference step size $\Delta t_{\text{ref}} = 2^{-14}$.

Figure 11 compares the cases where $\beta = 1$, $\alpha = 0.1$ in (a) and (b) and $\beta = 1$, $\alpha = 1$ in (c) and (d). When the linear term dominates (Figure 11 (a) and (b)) we see that the schemes *HomEI0* and *EI0* have smaller error and are the most efficient. In Figure 11 (c) and (d), where there is an equal weighting between the diagonal and nondiagonal term in the noise, we see *HomEI0* and *SETD0* are now equally efficient. When the nondiagonal part dominates the diagonal part of the noise then Figure 12 shows that *HomEI0* is still the most efficient closely followed by the semi-implicit Euler–Maruyama method.

4.4 *A finite difference discretisation of an SPDE*

Let us reconsider the reaction-diffusion equation (4.5) with homogeneous Dirichlet boundary conditions on (0,1). We now take space-time white noise so W(t) is Q- Wiener process on $L^2(0,1)$ with covariance $Q = I$. Introducing the grid points $x_j = jh$ for $h = 1/J$ and $j = 0,\ldots,J$, we denote the standard finite difference approximation of the Laplacian by A. Let $\mathbf{u}_J(t)$ be the solution of the SDE

$$d\mathbf{u_J} = [\varepsilon A\mathbf{u} + \mathbf{f}(\mathbf{u}_J)]\,dt + [\beta\mathbf{u}_J + \alpha\mathbf{g}(\mathbf{u}_J)]\,d\mathbf{W}_J(t) \tag{4.10}$$

where $\mathbf{f},\mathbf{g} : \mathbb{R}^{J-1} \to \mathbb{R}^{J-1}$ and $\mathbf{W}_J(t) = [W(t,x_1), W(t,x_2), ..., W(t,x_{J-1})]^T$. For this finite difference discretisation the commutator conditions (1.2) do not hold. So this example (like Section 4.3) is not covered by our theory, unlike the spectral Galerkin discretisation in Section 4.2. First consider the case of linear noise when $\alpha = 0$, in which case *HomEI0* and *EI0* are equivalent. We take $\beta = 0.5$, $T = 1$ $J = 101$ and $M = 1000$. We plot in Figure 13 the root mean square error (RMSE) against Δt in (a) and against cputime in (b). We see that we have an improved rate of convergence for *EI0* and that it is the most efficient of the schemes. When $\alpha = 0.125$, we include the presence of a nonlinear term in

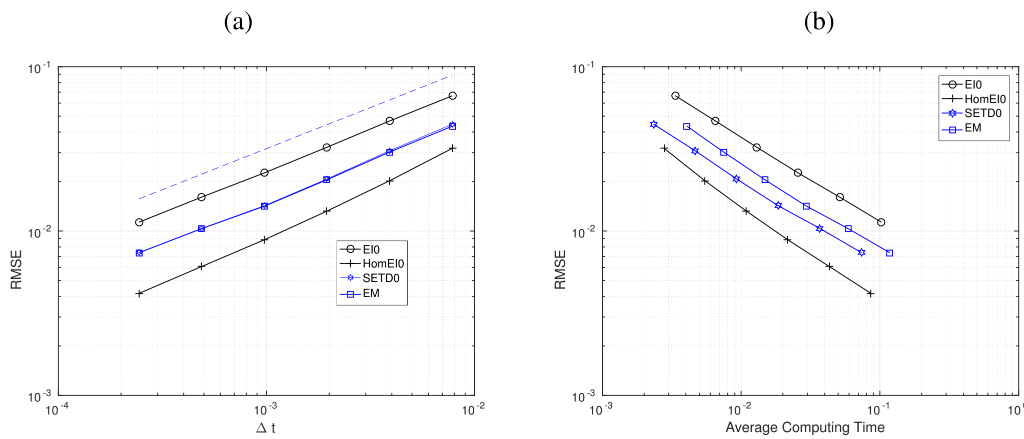

FIG. 7. Euler methods. Equation (4.6) with $\beta = 1$, $\alpha = 1$, $r = 4$, $T = 1$ and $M = 1000$ samples (a) root mean square error against Δt. Also plotted is a reference line with slope 1/2. (b) root mean square error against cputime. We have equal weighting of linear and nonlinear noise terms and we see *HomEI0* is clearly the most efficient and accurate. See Figure 8 for Milstein type schemes.

the noise, and results are shown in Figure 14. We still have an improved rate of convergence and now *HomEI0* is more slightly more accurate and efficient than *EI0*.

5. Proofs of the main results

Before giving the proofs of Theorems 3.1 and 3.2, we recall the following Proposition, see for example, Lord *et al.* (2014) for the proof.

PROPOSITION 5.1 Let Assumption 1 hold. For each $T > 0$ and $\mathbf{u}(0) = \mathbf{u}_0 \in \mathbb{R}^d$ there exists a unique $\mathbf{u}$ satisfying (1.1) such that

$$\sup_{t\in[0,T]} \|\mathbf{u}(t)\|_{L^2(\Omega,\mathbb{R}^d)} = \sup_{t\in[0,T]} \mathbb{E}\left[\|\mathbf{u}(t)\|_2^2\right]^{1/2} < \infty.$$

Furthermore, there exists $K > 0$ such that for $0 \leqslant s,t \leqslant T$

$$\|\mathbf{u}(t) - \mathbf{u}(s)\|_{L^2(\Omega,\mathbb{R}^d)} \leqslant K|t-s|^{1/2}. \tag{5.1}$$

LEMMA 5.1 The semigroup operator $\Phi_{t,s}$ given in (2) and $\Phi_{t,s}^{-1}$ satisfy the following : given $\mathbf{v} \in L^2(\Omega,\mathbb{R}^d)$

$$\|\Phi_{t,s}\mathbf{v}\|^2_{L^2(\Omega,\mathbb{R}^d)} \leqslant \mathbb{E}\left[\|\Phi_{t,s}\|_2^2\right] \|\mathbf{v}\|^2_{L^2(\Omega,\mathbb{R}^d)} \quad \text{and} \quad \left\|\Phi_{t,s}^{-1}\mathbf{v}\right\|^2_{L^2(\Omega,\mathbb{R}^d)} \leqslant \mathbb{E}\left[\left\|\Phi_{t,s}^{-1}\right\|_2^2\right] \|\mathbf{v}\|^2_{L^2(\Omega,\mathbb{R}^d)},$$

where $\|\Phi_{t,s}\|_2 = \sup_{\|\mathbf{x}\|_2=1} \|\Phi_{t,s}\mathbf{x}\|_2$ for $\mathbf{x} \in \mathbb{R}^d$. Furthermore,

$$\sup_{t,s\in[0,T]} \mathbb{E}\left[\|\Phi_{t,s}\|_2^2\right] < \infty \quad \text{and} \quad \sup_{t,s\in[0,T]} \mathbb{E}\left[\left\|\Phi_{t,s}^{-1}\right\|_2^2\right] < \infty.$$

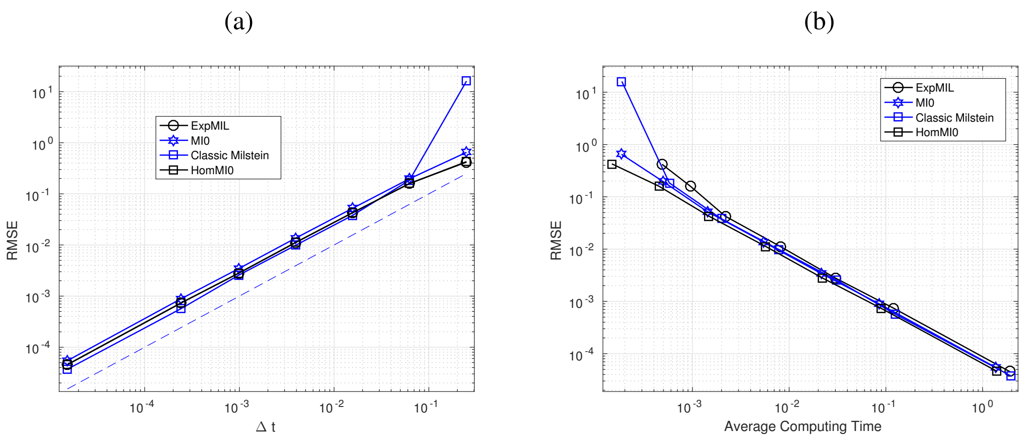

FIG. 8. Milstein methods. Equation (4.6) with $\beta = 1$, $\alpha = 1$, $r = 4$, $T = 1$ and $M = 100$ samples (a) root mean square error against Δt. Also plotted is a reference line with slope 1 (compare to Figure 7). In (b) root mean square error against cputime. With equal weighting of the noise we see *HomMI0* and *MI0* are marginally more efficient.

Proof.

Note that $\|\Phi_{t,s}\mathbf{v}\|_2^2 \leqslant \|\Phi_{t,s}\|_2^2\,\|\mathbf{v}\|_2^2$ and taking the expectation and applying the Cauchy– Schwarz inequality with the inequality $E[X^4] \leqslant E[X^2]^2$ (Pons, 2016) gives the first inequality. A straightforward calculation reveals

$$\mathbb{E}\left[\|\Phi_{t,s}\|_2^2\right] \leqslant e^{2\mathbb{E}\left[\left\|\left((A-\frac{1}{2}\sum_{i=1}^m B_i^2)(t-s)+\sum_{i=1}^m B_i(W_i(t)-W_i(s))\right)\right\|_2\right]}$$
$$\leqslant e^{2\left\|A-\frac{1}{2}\sum_{i=1}^m B_i^2\right\|_2|t-s|+2\sum_{i=1}^m\|B_i\|_2\sqrt{\frac{2|t-s|}{\pi}}},$$

which means that $\Phi_{t,s}$ and $\Phi_{t,s}^{-1}$ are uniformly bounded for $t,s \in [0,T]$. □

From now on we let

$$C = \max\left\{\sup_{s,t\in[0,T]} \mathbb{E}\left[\|\Phi_{s,t}\|_2^2\right],\ \sup_{s,t\in[0,T]} \mathbb{E}\left[\left\|\Phi_{s,t}^{-1}\right\|_2^2\right]\right\}.$$

We now start to examine the remainder terms that arise from the local error. Let us define the map for the exact flow

$$\Psi_{\text{Exact}}(t_{k+1},t_k,\mathbf{u}(t_k)) = \Phi_{t_{k+1},t_k}\left[\mathbf{u}(t_k) + \int_{t_k}^{t_{k+1}} \Phi_{s,t_k}^{-1}\tilde{\mathbf{f}}(\mathbf{u}(s))ds + \sum_{i=1}^m \int_{t_k}^{t_{k+1}} \Phi_{s,t_k}^{-1}\mathbf{g}_i(\mathbf{u}(s))dW_i(s)\right]. \quad (5.2)$$

This exact flow will be used in the analysis of *EI0*. However to analyse *MI0*, it is more convenient to use the following Ito-Taylor expansion (see (2.8))

$$\Psi_{\text{Exact}}(t_{k+1},t_k,\mathbf{u}(t_k)) = \Phi_{t_{k+1},t_k}\left[\mathbf{u}(t_k) + \int_{t_k}^{t_{k+1}} \Phi_{s,t_k}^{-1}\tilde{\mathbf{f}}(\mathbf{u}(s))ds + \sum_{i=1}^m \int_{t_k}^{t_{k+1}} \mathbf{g}_i(\mathbf{u}(t_k))dW_i(s)\right.$$
$$\left.+\sum_{i=1}^m\sum_{l=1}^m \int_{t_k}^{t_{k+1}}\int_{t_k}^{s} \Phi_{r,t_k}^{-1}\mathbf{H}_{i,l}(\mathbf{u}(r))dW_l(r)dW_i(s) + \sum_{i=1}^m \int_{t_k}^{t_{k+1}}\int_{t_k}^{s} \Phi_{r,t_k}^{-1}\mathbf{Q}_i(\mathbf{u}(r))drdW_i(s)\right]. \quad (5.3)$$

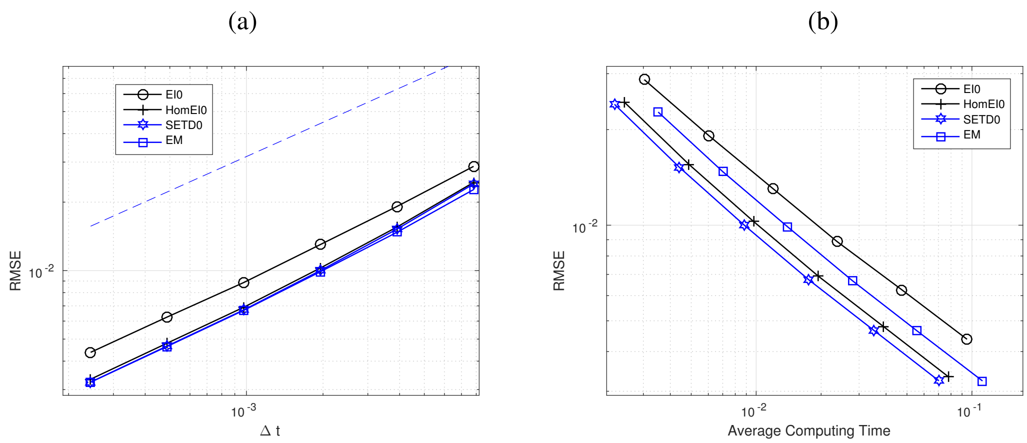

FIG. 9. Euler methods. Equation (4.6) with $\beta = 0.1$, $\alpha = 1$, $r = 4$, $T = 1$ and $M = 1000$ samples (a) root mean square error against Δt. Also plotted is a reference line with slope 1/2. (b) root mean square error against cputime. The noise is dominated by the nonlinear term. We now see that *SETD0* is the most efficient, followed by *HomEI0*. See Figure 10 for Milstein type schemes.

The numerical flows for *EI0* and *MI0* are given by

$$\Psi_{EI0}(t_{k+1},t_k,\mathbf{u}(t_k)) = \Phi_{t_{k+1},t_k}\mathbf{u}(t_k) + \Phi_{t_{k+1},t_k}\int_{t_k}^{t_{k+1}} \tilde{\mathbf{f}}(\mathbf{u}(t_k))ds + \sum_{i=1}^{m} \Phi_{t_{k+1},t_k}\int_{t_k}^{t_{k+1}} \mathbf{g}_i(\mathbf{u}(t_k))dW_i(s) \quad (5.4)$$

and

$$\Psi_{MI0}(t_{k+1},t_k,\mathbf{u}(t_k)) = \Psi_{EI0}(t_{k+1},t_k,\mathbf{u}(t_k)) + \sum_{i=1}^{m}\sum_{l=1}^{m} \Phi_{t_{k+1},t_k}\int_{t_k}^{t_{k+1}}\int_{t_k}^{s} \mathbf{H}_{i,l}(\mathbf{u}(t_k))dW_l(r)dW_i(s). \quad (5.5)$$

5.1 *Proof of Theorem 3.1*

First we look at the local error $R_{EI0} = \Psi_{\text{Exact}}(t,s,\mathbf{u}(s)) - \Psi_{EI0}(t,s,\mathbf{u}(s))$ for *EI0*.

LEMMA 5.2 Let Assumption 1 hold. Then

$$\left\| \sum_{k=0}^{N-1} \Phi_{t_N,t_{k+1}} R_{EI0}(t_{k+1},t_k,\mathbf{u}(t_k)) \right\|^2_{L^2(\Omega,\mathbb{R}^d)} = \mathcal{O}(\Delta t).$$

Proof. Considering the exact flow (5.2) and the numerical flow (5.4), the local error of *EI0* is given by

$$R_{EI0}(t_{k+1},t_k,\mathbf{u}(t_k)) = \Phi_{t_{k+1},t_k}\int_{t_k}^{t_{k+1}} \left(\Phi_{s,t_k}^{-1}\tilde{\mathbf{f}}(\mathbf{u}(s)) - \tilde{\mathbf{f}}(\mathbf{u}(t_k))\right) ds$$
$$+ \sum_{i=1}^{m} \Phi_{t_{k+1},t_k}\int_{t_k}^{t_{k+1}} \left(\Phi_{s,t_k}^{-1}\mathbf{g}_i(\mathbf{u}(s)) - \mathbf{g}_i(\mathbf{u}(t_k))\right) dW_i(s). \quad (5.6)$$

(a) (b)

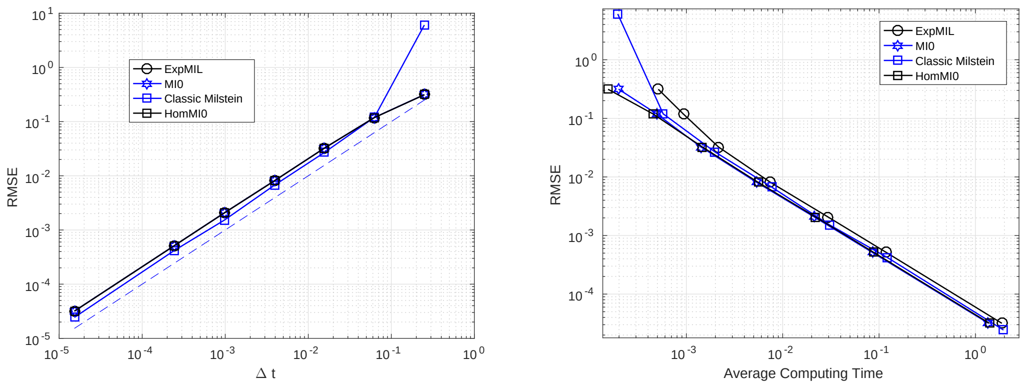

FIG. 10. Milstein methods. Equation (4.6) with $\beta = 0.1$, $\alpha = 1$, $r = 4$, $T = 1$ and $M = 100$ samples (a) root mean square error against Δt. Also plotted is a reference line with slope 1 (compare to Figure 9). In (b) root mean square error against cputime. The noise is dominated by the nonlinear term. We see that *HomMI0* and *MI0* are the most efficient.

Adding and subtracting the terms $\Phi_{s,t_k}^{-1}\tilde{\mathbf{f}}(\mathbf{u}(t_k))$ and $\Phi_{s,t_k}^{-1}\mathbf{g}_i(\mathbf{u}(t_k))$ in the first and second integrals we have

$$
\begin{aligned}
\left\| \sum_{k=0}^{N-1} \Phi_{t_N,t_{k+1}} R_{EI0}(t_{k+1},t_k,\mathbf{u}(t_k)) \right\|_{L^2(\Omega,\mathbb{R}^d)}^2 &\leqslant 4 \left\| \sum_{k=0}^{N-1} \Phi_{t_N,t_k} \int_{t_k}^{t_{k+1}} \Phi_{s,t_k}^{-1} \left(\tilde{\mathbf{f}}(\mathbf{u}(s)) - \tilde{\mathbf{f}}(\mathbf{u}(t_k)\right) ds \right\|_{L^2(\Omega,\mathbb{R}^d)}^2 \\
&+ 4 \left\| \sum_{k=0}^{N-1} \Phi_{t_N,t_k} \int_{t_k}^{t_{k+1}} \left(\Phi_{s,t_k}^{-1} \tilde{\mathbf{f}}(\mathbf{u}(t_k)) - \tilde{\mathbf{f}}(\mathbf{u}(t_k)\right) ds \right\|_{L^2(\Omega,\mathbb{R}^d)}^2 \\
&+ 4 \left\| \sum_{k=0}^{N-1} \Phi_{t_N,t_k} \sum_{i=1}^{m} \int_{t_k}^{t_{k+1}} \Phi_{s,t_k}^{-1} \left(\mathbf{g}_i(\mathbf{u}(s)) - \mathbf{g}_i(\mathbf{u}(t_k)) \right) dW_i(s) \right\|_{L^2(\Omega,\mathbb{R}^d)}^2 \\
&+ 4 \left\| \sum_{k=0}^{N-1} \Phi_{t_N,t_k} \sum_{i=1}^{m} \int_{t_k}^{t_{k+1}} \left(\Phi_{s,t_k}^{-1} \mathbf{g}_i(\mathbf{u}(t_k)) - \mathbf{g}_i(\mathbf{u}(t_k)) \right) dW_i(s) \right\|_{L^2(\Omega,\mathbb{R}^d)}^2 \\
&= I + II + III + IV.
\end{aligned}
$$

We now consider each of the terms I, II, III, IV separately. We start with I by applying Jensen's inequality for sums and Lemma 5.1

$$
\begin{aligned}
I &\leqslant 4N \sum_{k=0}^{N-1} \left\| \Phi_{t_N,t_k} \int_{t_k}^{t_{k+1}} \Phi_{s,t_k}^{-1} \left(\tilde{\mathbf{f}}(\mathbf{u}(s)) - \tilde{\mathbf{f}}(\mathbf{u}(t_k)\right) ds \right\|_{L^2(\Omega,\mathbb{R}^d)}^2 \\
&\leqslant 4NC \sum_{k=0}^{N-1} \mathbb{E} \left[\left\| \int_{t_k}^{t_{k+1}} \Phi_{s,t_k}^{-1} \left(\tilde{\mathbf{f}}(\mathbf{u}(s)) - \tilde{\mathbf{f}}(\mathbf{u}(t_k)\right) ds \right\|_2^2 \right].
\end{aligned}
$$

Now using Jensen's inequality for the integral, the global Lipschitz property of $\tilde{\mathbf{f}}$, Lemma 5.1 and Propo-

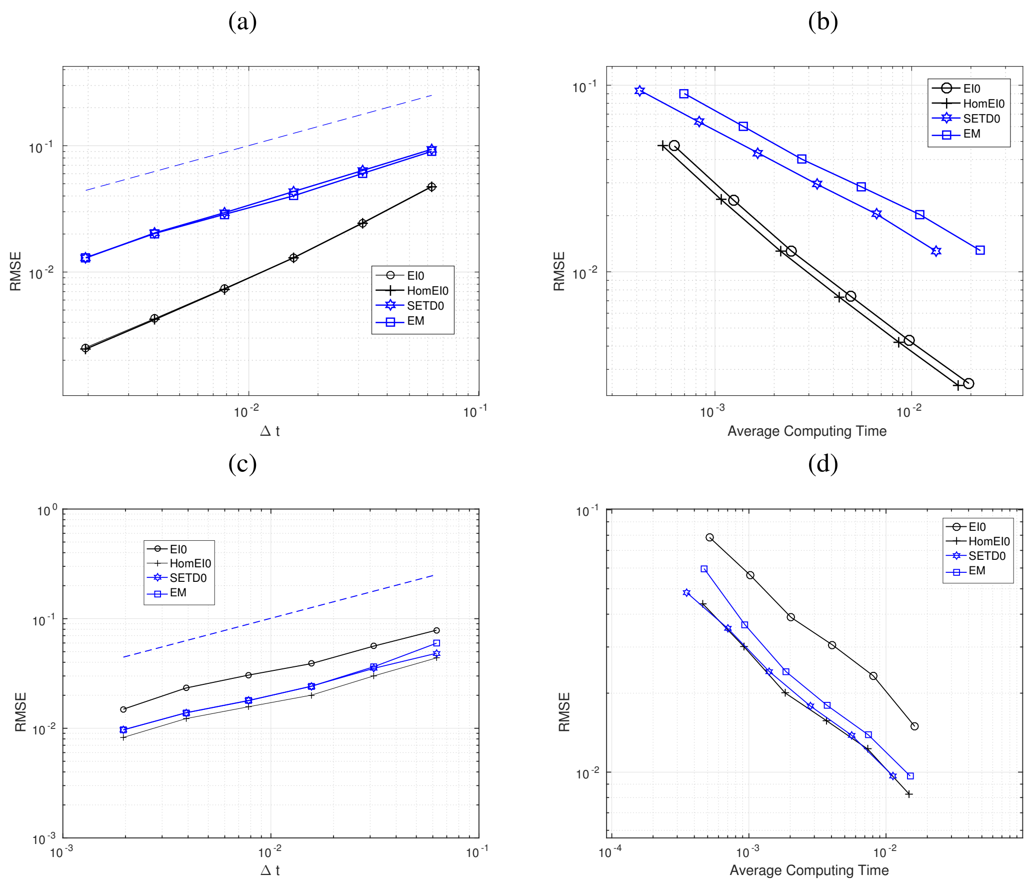

FIG. 11. Equation (4.6) with $r = 4$, $T = 1$ and $M = 100$ samples comparing in (a), (b) $\beta = 1$, $\alpha = 0.1$ and in (c), (d) $\beta = 1$, $\alpha = 1$. (a) and (c) show root mean square error against Δt. Also plotted is a reference line with slope 1/2. (b) and (d) root mean square error against cputime. Where the diagonal noise term dominates *HomEI0* is the most efficient. For equal weighting we see *HomEI0* is as efficient as *SETD0*.

sition 5.1 we get

$$
\begin{aligned}
I &\leqslant 4N\Delta t C \sum_{k=0}^{N-1} \int_{t_k}^{t_{k+1}} \mathbb{E}\left[\left\| \Phi_{s,t_k}^{-1} \left(\tilde{\mathbf{f}}(\mathbf{u}(s)) - \tilde{\mathbf{f}}(\mathbf{u}(t_k)) \right\|_2^2 \right] ds \\
&\leqslant 4TC^2L^2 \sum_{k=0}^{N-1} \int_{t_k}^{t_{k+1}} \mathbb{E}\left[\|(\mathbf{u}(s) - \mathbf{u}(t_k))\|_2^2 \right] ds \\
&\leqslant 4TC^2L^2K^2 \sum_{k=0}^{N-1} \int_{t_k}^{t_{k+1}} |s - t_k| ds = K_I \Delta t.
\end{aligned}
$$

For II, it is straightforward to see $II \leqslant K_{II}\Delta t$ by considering the fact that $\mathbb{E}\left[\left\| \left(\Phi_{s,t_k}^{-1} - I \right) \mathbf{v} \right\|_2^2 \right] \leqslant K|s - t_k|$

(a) (b)

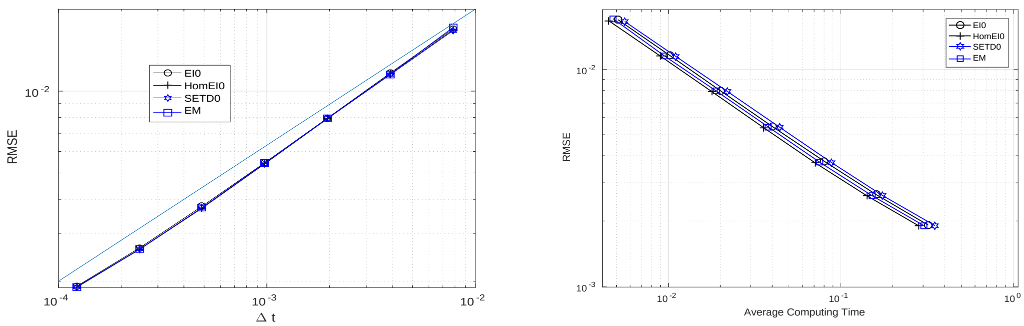

FIG. 12. Equation (4.6) with $r = 4$, $T = 1$ and $M = 1000$ samples with $\beta = 0.1$, $\alpha = 1$. (a) root mean square error against Δt. Also plotted is a reference line with slope 1/2. (b) root mean square error against cputime. The noise is dominated by the non diagonal term and we now see that *HomEI0* is the most efficient, followed by the semi-implicit Euler–Maruyama method.

for any $\mathscr{F}_{t_k}$ measurable $\mathbf{v} \in L^2(\Omega, \mathbb{R}^d)$. This follows since $\mathbf{u}(t) = \Phi_{s,t_k}^{-1}\mathbf{v}$ is the solution of the SDE

$$d\mathbf{u} = (-A + \sum_{i=1}^{m} B_i)\mathbf{u}(t)dt - \sum_{i=1}^{m} B_i \mathbf{u}(t) dW_i(t), \qquad \mathbf{u}(t_k) = \mathbf{v}$$

satisfying assumptions of Proposition 5.1.

For the term III,

$$III = 4 \left\| \Phi_{t_N,0} \sum_{k=0}^{N-1} \sum_{i=1}^{m} \int_{t_k}^{t_{k+1}} \Phi_{s,0}^{-1} \left(\mathbf{g}_i(\mathbf{u}(s)) - \mathbf{g}_i(\mathbf{u}(t_k)) \right) dW_i(s) \right\|_{L^2(\Omega,\mathbb{R}^d)}^2$$

where $\Phi_{t_N,t_k} = \Phi_{t_N,0}\Phi_{t_k,0}^{-1}$ is due to commutativity of the matrices A and B_i, $i = 1, \ldots, m$. We have by the Ito isometry

$$\begin{aligned} III &\leqslant 4C \sum_{k=0}^{N-1} \sum_{i=1}^{m} \int_{t_k}^{t_{k+1}} \mathbb{E}\left[\left\| \Phi_{s,0}^{-1} \left(\mathbf{g}_i(\mathbf{u}(s)) - \mathbf{g}_i(\mathbf{u}(t_k)) \right) \right\|_2^2 \right] ds \\ &\leqslant 4C^2 L^2 K^2 m \sum_{k=0}^{N-1} \int_{t_k}^{t_{k+1}} |s - t_k| ds = \mathscr{O}(\Delta t) \end{aligned}$$

where the global Lipschitz property of $\mathbf{g}_i$, Proposition 5.1, and Lemma 5.1 are used. By a similar argument we have $IV = \mathscr{O}(\Delta t)$. Combining I, II, III and IV we obtain the result. □

Proof of Theorem 3.1. By induction, we can express the approximation of $\mathbf{u}(t_N)$ by $\mathbf{u}_N$ found by *EI0* at $t = t_N$ as

$$\mathbf{u}_N = \Phi_{t_N,0}\mathbf{u}_0 + \sum_{k=0}^{N-1} \Phi_{t_N,t_k} \int_{t_k}^{t_{k+1}} \tilde{\mathbf{f}}(\mathbf{u}_k) ds + \sum_{k=0}^{N-1} \sum_{i=1}^{m} \Phi_{t_N,t_k} \int_{t_k}^{t_{k+1}} \mathbf{g}_i(\mathbf{u}_k) dW_i(s). \tag{5.7}$$

Due to commutativity of the matrices A and B_i's, $\Phi_{t_N,t_k} = \Phi_{t_N,0}\Phi_{t_k,0}^{-1}$, the matrix $\Phi_{t_k,0}^{-1}$ can be taken

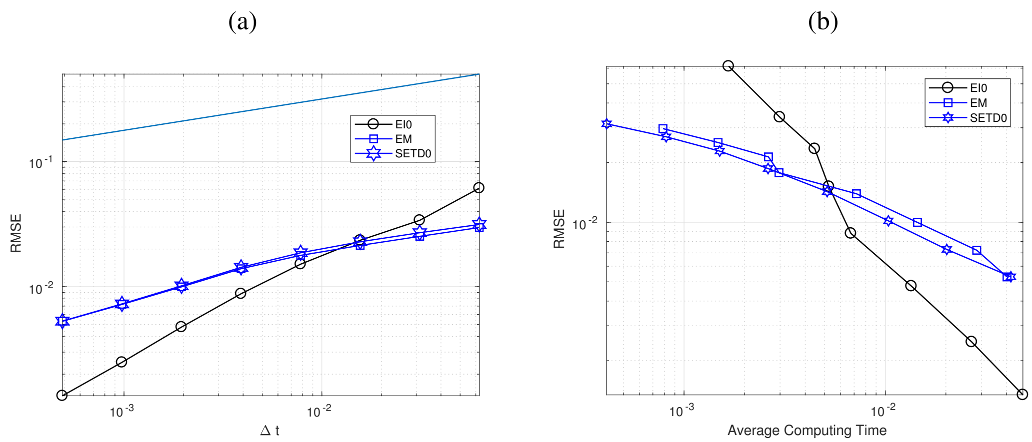

FIG. 13. Euler methods for (4.10) with $\beta = 0.5$, $\alpha = 0$, $T = 1$ and $M = 1000$ samples (a) root mean square error against Δt. Also plotted is a reference line with slope 1/2. In (b) we examine efficiency. We see that *EI0* has an improved rate of convergence and is the most efficient even though commutator conditions (1.2) do not hold. See Figure 14 for $\alpha > 0$.

inside the integrals. Now we define the continuous time process $\mathbf{u}_{\Delta t}(t)$ for (5.7) that agrees with approximation $\mathbf{u}_k$ at $t = t_k$. By introducing the variable $\hat{t} = t_k$ for $t_k \leqslant t < t_{k+1}$,

$$\mathbf{u}_{\Delta t}(t) = \Phi_{t,0}\mathbf{u}_{\Delta t}(0) + \Phi_{t,0}\int_0^t \Phi_{\hat{s},0}^{-1}\tilde{\mathbf{f}}(\mathbf{u}_{\Delta t}(\hat{s}))ds + \sum_{i=1}^m \Phi_{t,0}\int_0^t \Phi_{\hat{s},0}^{-1}\mathbf{g}_i(\mathbf{u}_{\Delta t}(\hat{s}))dW_i(s).$$

This continuous version has the property that $\mathbf{u}_{\Delta t}(t_k) = \mathbf{u}_k$. By recalling the definition of the local error, the iterated sum of the exact solution at $t = t_N$ is found by induction to be

$$\begin{aligned}\mathbf{u}(t_N) = \Phi_{t_N,0}\mathbf{u}_0 + \Phi_{t_N,0}\int_0^{t_N} \Phi_{\hat{s},0}^{-1}\tilde{\mathbf{f}}(\mathbf{u}(\hat{s}))ds \\ + \Phi_{t_N,0}\sum_{i=1}^m \int_0^{t_N} \Phi_{\hat{s},0}^{-1}\mathbf{g}_i(\mathbf{u}(\hat{s}))dW_i(s) + \sum_{k=0}^{N-1}\Phi_{t_N,t_{k+1}}R_{EI0}(t_{k+1},t_k,\mathbf{u}(t_k)).\end{aligned} \tag{5.8}$$

Denoting the error by $\mathbf{e}(\hat{t}) = \mathbf{u}(\hat{t}) - \mathbf{u}_{\Delta t}(\hat{t})$, we see that

$$\|\mathbf{e}(\hat{t})\|^2_{L^2(\Omega,\mathbb{R}^d)} \leqslant \left(3\hat{t}C^2L^2 + 3C^2mL^2\right)\int_0^{\hat{t}} \mathbb{E}\left[\|\mathbf{e}(s)\|_2^2\right]ds + 3K_{EI0}\Delta t,$$

where L is the largest one of the Lipschitz constants of the functions $\mathbf{g}_i$, $\tilde{\mathbf{f}}$. Finally, Gronwall's inequality completes the proof.

5.2 *Proof of Theorem 3.2*

We now examine the local error for *MI0*, given by (2.11).

LEMMA 5.3 Let Assumptions 1 and 2 and 3 hold. Then

$$\left\|\sum_{k=0}^{N-1}\Phi_{t_N,t_k+1}R_{MI0}(t_{k+1},t_k,\mathbf{u}(t_k))\right\|^2_{L^2(\Omega,\mathbb{R}^d)} = \mathscr{O}(\Delta t^2) \tag{5.9}$$

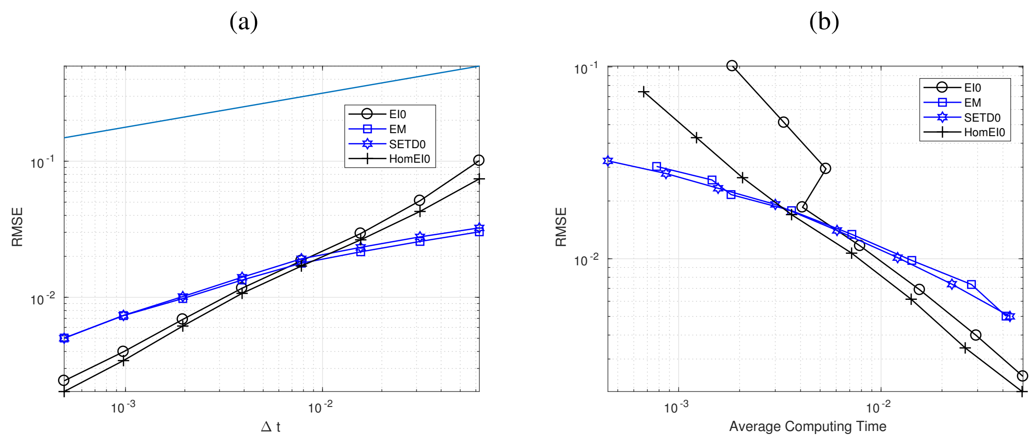

FIG. 14. Euler methods for (4.10) with $\beta = 0.5$, $\alpha = 0.125$, $T = 1$ and $M = 1000$ samples (a) root mean square error (RMSE) against Δt. Also plotted is a reference line with slope 1/2. (b) RMSE against cputime. We see that *EI0* and *HomEI0* have an improved rate of convergence and are the most efficient. See Figure 13 for $\alpha = 0$.

where $R_{MI0}(t,s,\mathbf{u}(s)) = \Psi_{\text{Exact}}(t,s,\mathbf{u}(s)) - \Psi_{MI0}(t,s,\mathbf{u}(s))$.

Proof. Considering the exact flow (5.3) and the numerical flow (5.5) corresponding to the scheme *MI0*, we have

$$\begin{aligned} R_{MI0}(t_{k+1},t_k,\mathbf{u}(t_k)) &= \Phi_{t_{k+1},t_k} \int_{t_k}^{t_{k+1}} \left(\Phi_{s,t_k}^{-1} \tilde{\mathbf{f}}(\mathbf{u}(s)) - \tilde{\mathbf{f}}(\mathbf{u}(t_k)) \right) ds \\ &\quad + \sum_{i=1}^{m} \sum_{l=1}^{m} \Phi_{t_{k+1},t_k} \int_{t_k}^{t_{k+1}} \int_{t_k}^{s} \left(\Phi_{r,t_k}^{-1} \mathbf{H}_{i,l}(\mathbf{u}(r)) - \mathbf{H}_{i,l}(\mathbf{u}(t_k)) \right) dW_l(r) dW_i(s) \\ &\quad + \sum_{i=1}^{m} \Phi_{t_{k+1},t_k} \int_{t_k}^{t_{k+1}} \int_{t_k}^{s} \Phi_{r,t_k}^{-1} \mathbf{Q}_i(\mathbf{u}(r)) dr dW_i(s). \qquad (5.10) \end{aligned}$$

Adding and subtracting the terms $\Phi_{s,t_k}^{-1}\tilde{\mathbf{f}}(\mathbf{u}(t_k))$, $\Phi_{s,t_k}^{-1}\mathbf{H}_{i,l}(\mathbf{u}(t_k))$ in the first and second integrals respectively and summing and taking the norm and applying Jensen's inequality, we have

$$\left\| \sum_{k=0}^{N-1} \Phi_{t_N,t_{k+1}} R_{MI0}(t_{k+1},t_k,\mathbf{u}(t_k)) \right\|_{L^2(\Omega,\mathbb{R}^d)}^2 \leqslant I + II + III + IV + V$$

with

$$I := 5 \left\| \sum_{k=0}^{N-1} \Phi_{t_N,t_k} \int_{t_k}^{t_{k+1}} \Phi_{s,t_k}^{-1} \left(\tilde{\mathbf{f}}(\mathbf{u}(s)) - \tilde{\mathbf{f}}(\mathbf{u}(t_k)) \right) ds \right\|_{L^2(\Omega,\mathbb{R}^d)}^2$$

$$II := 5 \left\| \sum_{k=0}^{N-1} \Phi_{t_N,t_k} \int_{t_k}^{t_{k+1}} \left(\Phi_{s,t_k}^{-1} \tilde{\mathbf{f}}(\mathbf{u}(t_k)) - \tilde{\mathbf{f}}(\mathbf{u}(t_k)) \right) ds \right\|_{L^2(\Omega,\mathbb{R}^d)}^2$$

$$III := 5 \left\| \sum_{k=0}^{N-1} \sum_{i=1}^{m} \sum_{l=1}^{m} \Phi_{t_N,t_k} \int_{t_k}^{t_{k+1}} \int_{t_k}^{s} \Phi_{r,t_k}^{-1} \left(\mathbf{H}_{i,l}(\mathbf{u}(r)) - \mathbf{H}_{i,l}(\mathbf{u}(t_k)) \right) dW_l(r) dW_i(s) \right\|_{L^2(\Omega,\mathbb{R}^d)}^2$$

$$IV := 5\left\|\sum_{k=0}^{N-1}\sum_{i=1}^{m}\sum_{l=1}^{m}\Phi_{t_N,t_k}\int_{t_k}^{t_{k+1}}\int_{t_k}^{s}\left(\Phi_{r,t_k}^{-1}\mathbf{H}_{i,l}(\mathbf{u}(t_k))-\mathbf{H}_{i,l}(\mathbf{u}(t_k))\right)dW_l(r)dW_i(s)\right\|_{L^2(\Omega,\mathbb{R}^d)}^2$$

and remainder

$$V =: 5\left\|\sum_{k=0}^{N-1}\sum_{i=1}^{m}\Phi_{t_N,t_k}\int_{t_k}^{t_{k+1}}\int_{t_k}^{s}\Phi_{r,t_k}^{-1}\mathbf{Q}_i(\mathbf{u}(r))drdW_i(s)\right\|_{L^2(\Omega,\mathbb{R}^d)}^2.$$

We now consider each of the terms I, II, III, IV, V separately and we start with I. By Assumption 3, we have the following Ito-Taylor expansion for $\tilde{\mathbf{f}}$

$$\begin{aligned}\tilde{\mathbf{f}}(\mathbf{u}(\mathbf{s})) &= \tilde{\mathbf{f}}(\mathbf{u}(t_k))+\sum_{i=1}^{m}D\tilde{\mathbf{f}}(\mathbf{u}(t_k))\left(B_i\mathbf{u}(t_k)+\mathbf{g}_i(\mathbf{u}(t_k))\right)\left(W_i(s)-W_i(t_k)\right)+R_{\tilde{f}}\\ &= \tilde{\mathbf{f}}(\mathbf{u}(t_k))+\sum_{i=1}^{m}\mathbf{K}_i\left(W_i(s)-W_i(t_k)\right)+R_{\tilde{f}}.\end{aligned}$$

We know that $R_{\tilde{f}} = \mathscr{O}(s-t_k)$, see for example Lord *et al.* (2014). By Jensen's inequality for the sum and Ito-Taylor expansion,

$$\begin{aligned}I \leqslant & 10\mathbb{E}\left[\left\|\sum_{k=0}^{N-1}\int_{t_k}^{t_{k+1}}\Phi_{t_N,s}\left(\sum_{i=1}^{m}\mathbf{K}_i\left(W_i(s)-W_i(t_k)\right)\right)ds\right\|_2^2\right]\\ &+10\mathbb{E}\left[\left\|\sum_{k=0}^{N-1}\int_{t_k}^{t_{k+1}}\Phi_{t_N,s}R_{\tilde{f}}ds\right\|_2^2\right].\end{aligned}$$

By Lemma 5.1 for $\Phi_{t_N,s}$, we have

$$I \leqslant 10C\mathbb{E}\left[\left\|\sum_{k=0}^{N-1}\int_{t_k}^{t_{k+1}}\left(\sum_{i=1}^{m}\mathbf{K}_i\left(W_i(s)-W_i(t_k)\right)\right)ds\right\|_2^2\right]+10C\mathbb{E}\left[\left\|\sum_{k=0}^{N-1}\int_{t_k}^{t_{k+1}}R_{\tilde{f}}ds\right\|_2^2\right].$$

Let us write $I \leqslant I_a + I_b$, representing the first and second term by I_a and I_b respectively, and investigate the first term I_a. By the orthogonality relation $\mathbb{E}\left[<\Theta_k, \Theta_l>\right] = 0$, $k \neq l$ for

$$\Theta_k = \int_{t_k}^{t_{k+1}}\left(\sum_{i=1}^{m}\mathbf{K}_i\left(W_i(s)-W_i(t_k)\right)\right)ds,$$

we have

$$I_a = 10C\sum_{k=0}^{N-1}\mathbb{E}\left[\left\|\int_{t_k}^{t_{k+1}}\left(\sum_{i=1}^{m}\mathbf{K}_i\left(W_i(s)-W_i(t_k)\right)\right)ds\right\|_2^2\right].$$

By two applications of Jensen's inequality for the integral and sum

$$I_a \leqslant 10CmK\Delta t\sup_{i\in\{1\ldots m\}}\mathbb{E}\left[\|\mathbf{K}_i\|_2\right]^2\sum_{k=0}^{N-1}\sum_{i=1}^{m}\int_{t_k}^{t_{k+1}}\mathbb{E}\left[\|W_i(s)-W_i(t_k)\|_2^2\right]ds = \mathscr{O}(\Delta t^2).$$

Since R_f contains higher order terms, we conclude $I = \mathscr{O}(\Delta t^2)$. Similarly, for II we find the same order by following same arguments.

For III, we have by the Ito isometry applied consecutively for outer and inner stochastic integrals

$$\begin{aligned} III \leqslant & 5C \left\| \sum_{k=0}^{N-1} \sum_{i=1}^{m} \sum_{l=1}^{m} \int_{t_k}^{t_{k+1}} \int_{t_k}^{s} \Phi_{r,0}^{-1} \left(\mathbf{H}_{i,l}(\mathbf{u}(r)) - \mathbf{H}_{i,l}(\mathbf{u}(t_k)) \right) dW_l(r) dW_i(s) \right\|_{L^2(\Omega,\mathbb{R}^d)}^2 \\ &= 5C \sum_{k=0}^{N-1} \sum_{i=1}^{m} \int_{t_k}^{t_{k+1}} \mathbb{E} \left[\left\| \left(\sum_{l=1}^{m} \int_{t_k}^{s} \Phi_{r,0}^{-1} \left(\mathbf{H}_{i,l}(\mathbf{u}(r)) - \mathbf{H}_{i,l}(\mathbf{u}(t_k)) \right) dW_l(r) \right) \right\|_2^2 \right] ds \\ &= 5C \sum_{k=0}^{N-1} \sum_{i=1}^{m} \sum_{l=1}^{m} \int_{t_k}^{t_{k+1}} \int_{t_k}^{s} \mathbb{E} \left[\left\| \Phi_{r,0}^{-1} \left(\mathbf{H}_{i,l}(\mathbf{u}(r)) - \mathbf{H}_{i,l}(\mathbf{u}(t_k)) \right) \right\|_2^2 \right] dr ds. \end{aligned}$$

By the global Lipschitz property of $\mathbf{H}_{i,l}$, Proposition 5.1 and Lemma 5.1

$$III \leqslant K_{III} \sum_{k=0}^{N-1} \int_{t_k}^{t_{k+1}} \int_{t_k}^{s} |r - t_k| dr ds = K_{III} \Delta t^2.$$

In a similar way, it can be shown that $IV \leqslant K_{IV} \Delta t^2$. Since $\int_{t_k}^{t_{k+1}} \int_{t_k}^{s} dr dW(s) \sim N(0, \frac{1}{3}\Delta t^3)$, it is straightforward to see $V \leqslant K_V \Delta t^2$. □

Proof of Theorem 3.2 As in the proof of Theorem 3.1, we define the continuous time process $\mathbf{u}_{\Delta t}(t)$ for *MI0* that agrees with approximation $\mathbf{u}_k$ at $t = t_k$. By introducing the variable $\hat{t} = t_k$ for $t_k \leqslant t < t_{k+1}$,

$$\begin{aligned} \mathbf{u}_{\Delta t}(t) = \Phi_{t,0} \mathbf{u}_{\Delta t}(0) + \Phi_{t,0} \int_0^t \Phi_{\hat{s},0}^{-1} \tilde{\mathbf{f}}(\mathbf{u}_{\Delta t}(\hat{s})) ds + \sum_{i=1}^{m} \Phi_{t,0} \int_0^t \Phi_{\hat{s},0}^{-1} \mathbf{g}_i(\mathbf{u}_{\Delta t}(\hat{s})) dW_i(s) \\ + \sum_{i=1}^{m} \sum_{l=1}^{m} \Phi_{t,0} \int_0^t \int_{\hat{s}}^{s} \Phi_{\hat{s},0}^{-1} \mathbf{H}_{i,l}(\mathbf{u}_{\Delta t}(\hat{s})) dW_l(r) dW_i(s). \end{aligned} \tag{5.11}$$

The iterated sum of the exact solution at $t = t_N$ is obtained inductively to be

$$\begin{aligned} \mathbf{u}(t_N) = \Phi_{t_N,0} \mathbf{u}_0 + \Phi_{t_N,0} \int_0^{t_N} \Phi_{\hat{s},0}^{-1} \tilde{\mathbf{f}}(\mathbf{u}(\hat{s})) ds + \Phi_{t_N,0} \sum_{i=1}^{m} \int_0^{t_N} \Phi_{\hat{s},0}^{-1} \mathbf{g}_i(\mathbf{u}(\hat{s})) dW_i(s) \\ + \sum_{i=1}^{m} \sum_{l=1}^{m} \Phi_{t_N,0} \int_0^{t_N} \int_{\hat{s}}^{s} \Phi_{\hat{s},0}^{-1} \mathbf{H}_{i,l}(\mathbf{u}(\hat{s})) dW_l(r) dW_i(s) + \sum_{k=0}^{N-1} \Phi_{t_N,t_{k+1}} R_{MI0}(t_{k+1}, t_k, \mathbf{u}(t_k)). \end{aligned} \tag{5.12}$$

Denoting the error by $\mathbf{e}(\hat{t}) = \mathbf{u}(\hat{t}) - \mathbf{u}_{\Delta t}(\hat{t})$, we see that

$$\|\mathbf{e}(\hat{t})\|_{L^2(\Omega,\mathbb{R}^d)}^2 \leqslant \left(4\hat{t}C^2L^2 + 4C^2L^2m(1+m)\right) \int_0^{\hat{t}} \mathbb{E}\left[\|\mathbf{e}(s)\|_2^2\right] ds + 4K_{MI0}\Delta t^2.$$

Finally, Gronwall's inequality completes the proof.

6. Conclusion and remarks

Exponential integrators that take advantage of the exact solution of Geometric Brownian Motion have been derived and strong convergence proved. Weak convergence of these numerical methods is under investigation and numerically we observe convergence of $\mathscr{O}(\Delta t)$ (as would be expected). The proposed schemes are particularly well suited to SDEs arising from the spectral Galerkin discretisation of a SPDE, see Section 4.2, where typically diagonal noise arises and the zero commutator conditions (1.2) hold. The homotopy based scheme we introduced can take advantage of linearity in the diffusion and at the same time effectively handle nonlinear noise. Where the SDEs are not of the semi-linear form of (1.1) then a Rosenbrock type method could be applied, similar to Hochbruck *et al.* (2009). The numerical results of Section 4.3 and Section 4.4 examine cases where the zero commutator conditions fail. Our numerical examples show that these new exponential based schemes remain more efficient than the standard integrators.

We have seen in this work the effectiveness of the homotopy approach with the simple choice of parameter in (4.2) and it would be interesting to investigate an adaptive choice in the future, preliminary work suggests that this can further increase the efficiency.

Acknowledgements

The first author was supported by Tubitak grant : 2219 International Post-Doctoral Research Fellowship Programme. Work was completed at the Department of Mathematics, Maxwell Institute, Heriot Watt University, UK whilst on leave from the Department of Mathematics, Uşak University, Turkey. We would like to thank Raphael Kruse for his comments on an earlier draft.

REFERENCES

BECKER, S., JENTZEN, A. & KLOEDEN, P. (2016) An exponential Wagner–Platen type scheme for spdes. *SIAM J. Numer. Anal.*

BISCAY, R., JIMENEZ, J., RIERA, J. & VALDES, P. (1996) Local linearization method for the numerical solution of stochastic differential equations. *Annals of the Institute of Statistical Mathematics*, **48**, 631–644.

BUCKWAR, E. & KELLY, C. (2010) Towards a systematic linear stability analysis of numerical methods for systems of stochastic differential equations. *SIAM J. Numer. Anal.*, **48**, 298–321.

CARBONELL, F. & JIMENEZ, J. C. (2008) Weak local linear discretizations for stochastic differential equations with jumps. *J. Appl. Probab.*, **45**, 201–210.

HASEGAWA, H. (2008) Stochastic bifurcation in FitzHugh-Nagumo ensembles subjected to additive and/or multiplicative noises. *Physica D: Nonlinear Phenomena*, **237**, 137 – 155.

HOCHBRUCK, M., OSTERMANN, A. & SCHWEITZER, J. (2009) Exponential Rosenbrock-type methods. *SIAM Journal on Numerical Analysis*, **47**, 786–803.

HOCHBRUCK, M. & OSTERMANN, A. (2010) Exponential integrators. *Acta Numerica*, **19**, 209–286.

HUTZENTHALER, M. & JENTZEN, A. (2015) *Numerical approximations of stochastic differential equations with non-globally Lipschitz continuous coefficients*, vol. 236. American Mathematical Society.

JENTZEN, A. (2009) Pathwise numerical approximation of SPDEs with additive noise under non-global Lipschitz coefficients. *Potential Anal.*, **31**, 375–404.

JENTZEN, A. (2010) Taylor expansions of solutions of stochastic partial differential equations. *Discrete Contin. Dyn. Syst. Ser. B*, **14**, 515–557.

JENTZEN, A. & KLOEDEN, P. E. (2009) Overcoming the order barrier in the numerical approximation of stochastic partial differential equations with additive space-time noise. *Proc. R. Soc. Lond. Ser. A Math. Phys. Eng. Sci.*, **465**, 649–667.

JENTZEN, A. & RÖCKNER, M. (2015) A Milstein scheme for SPDEs. *Foundations of Computational Mathematics*, **15**, 313–362.

JIMENEZ, J., SHOJI, I. & OZAKI, T. (1999) Simulation of stochastic differential equations through the local linearization method. a comparative study. *Journal of Statistical Physics*, **94**, 587–602.

JIMENEZ, J. C. & CARBONELL, F. (2015) Convergence rate of weak local linearization schemes for stochastic differential equations with additive noise. *J. Comput. Appl. Math.*, **279**, 106–122.

KLOEDEN, P. E., LORD, G. J., NEUENKIRCH, A. & SHARDLOW, T. (2011) The exponential integrator scheme for stochastic partial differential equations: Pathwise error bounds. *Journal of Computational and Applied Mathematics*, **235**, 1245–1260.

KLOEDEN, P. & PLATEN, E. (2011) *Numerical Solution of Stochastic Differential Equations*. Stochastic Modelling and Applied Probability. Springer Berlin Heidelberg.

KOMORI, Y. & BURRAGE, K. (2014) A stochastic exponential Euler scheme for simulation of stiff biochemical reaction systems. *BIT*, **54**, 1067–1085.

LI, X., JIANG, D. & MAO, X. (2009) Population dynamical behavior of Lotka–Volterra system under regime switching. *Journal of Computational and Applied Mathematics*, **232**, 427 – 448.

LORD, G. J., POWELL, C. E. & SHARDLOW, T. (2014) *An Introduction to Computational Stochastic PDEs*. Cambridge University Press.

LORD, G. J. & ROUGEMONT, J. (2004) A numerical scheme for stochastic PDEs with Gevrey regularity. *IMA J. Numer. Anal.*, **24**, 587–604.

LORD, G. J. & TAMBUE, A. (2012) Stochastic exponential integrators for the finite element discretization of SPDEs for multiplicative and additive noise. *IMA J. Numer. Anal.*, drr059.

MAO, X. (1997) *Stochastic differential equations and their applications*. Horwood Publishing Series in Mathematics & Applications. Horwood Publishing Limited, Chichester, pp. xii+366.

MORA, C. M. (2005) Weak exponential schemes for stochastic differential equations with additive noise. *IMA J. Numer. Anal.*, **25**, 486–506.

ØKSENDAL, B. (2003) Stochastic differential equations. *Stochastic differential equations*. Springer, pp. 65–84.

PONS, O. (2016) *Inequalities in analysis and probability*. World Scientific.

SAITO, Y. & MITSUI, T. (1996) Stability analysis of numerical schemes for stochastic differential equations. *SIAM Journal on Numerical Analysis*, **33**, 2254–2267.